JOURNAL OF SYNCHROTRON RADIATION

ISSN 1600-5775

Received 8 September 2017
Accepted 29 September 2017

Edited by A. Momose, Tohoku University, Japan

Keywords: phase contrast imaging; portal vein embolization; CO_2 microbubbles.

Phase contrast imaging of preclinical portal vein embolization with CO_2 microbubbles

Rongbiao Tang,[a]* Fuhua Yan,[a] Guo-Yuan Yang[b] and Ke-Min Chen[a]*

[a]Department of Radiology, Rui Jin Hospital, Shanghai Jiao Tong University School of Medicine, Shanghai 200025, People's Republic of China, and [b]Neuroscience and Neuroengineering Center, Med-X Research Institute, Shanghai Jiao Tong University School of Medicine, Shanghai 200030, People's Republic of China. *Correspondence e-mail: tangme8688258@sina.com, keminchenrj@163.com

Preoperative portal vein embolization (PVE) is employed clinically to avoid postoperative liver insufficiency. Animal models are usually used to study PVE in terms of mechanisms and pathophysiological changes. PVE is formerly monitored by conventional absorption contrast imaging (ACI) with iodine contrast agent. However, the side effects induced by iodine can give rise to animal damage and death. In this study, the feasibility of using phase contrast imaging (PCI) to show PVE using homemade CO_2 microbubbles in living rats has been investigated. CO_2 gas was first formed from the reaction between citric acid and sodium bicarbonate. The CO_2 gas was then encapsulated by egg white to fabricate CO_2 microbubbles. ACI and PCI of CO_2 microbubbles were performed and compared *in vitro*. An additional increase in contrast was detected in PCI. PCI showed that CO_2 microbubbles gradually dissolved over time, and the remaining CO_2 microbubbles became larger. By PCI, the CO_2 microbubbles were found to have certain stability, suggesting their potential use as embolic agents. CO_2 microbubbles were injected into the main portal trunk to perform PVE in living rats. PCI exploited the differences in the refractive index and facilitated clear visualization of the PVE after the injection of CO_2 microbubbles. Findings from this study suggest that homemade CO_2 microbubbles-based PCI is a novel modality for preclinical PVE research.

1. Introduction

Portal vein embolization (PVE) is a valuable utility for inducing hepatic lobe hypertrophy before surgery (Furrer *et al.*, 2008; Omichi *et al.*, 2017). Basic research on PVE has generally been carried out in animal models at the preclinical stage. PVE with embolic agents has previously been performed under the guidance of X-ray-based digital subtraction angiography (DSA). Because the difference between the absorption coefficients of blood-filled portal veins and liver parenchyma is small, iodine is generally used as a contrast agent when performing DSA. However, iodine can trigger an allergic reaction, which will induce nephrotoxicity and hepatotoxicity. These side effects can give rise to injury and death of the animal models. Therefore, a novel imaging modality should be utilized for preclinical PVE research.

Conventional absorption contrast imaging (ACI) generates contrast based on X-ray attenuation by an object. However, owing to its weak absorption, soft tissue is often not visible using ACI. Besides absorption, phase shift is another contrast mechanism between X-rays and tissue (Thüring *et al.*, 2014). Currently, synchrotron radiation (SR) phase contrast imaging (PCI) is widely used to present superb image contrast for soft tissue (Bravin *et al.*, 2013; Lewis, 2004; Miklos *et al.*, 2015; Tang *et al.*, 2012). Vessels in dehydrated liver down to the micro-

meter level have been noticeably detected by PCI using air as a contrast agent (Laperle *et al.*, 2008; Xuan *et al.*, 2015; Zhang *et al.*, 2008). Additionally, in our previous study (Tang *et al.*, 2012), PCI was shown to clearly detect embolic agents in portal veins without the dehydration process. Therefore, iodine can be avoided when using PCI. However, these studies could only be applied to image excised samples.

In this study, we have fabricated CO_2 microbubbles and used them as embolic agents for PVE. The feasibility of using PCI for imaging PVE with CO_2 microbubbles in living rats is evaluated.

2. Materials and methods

2.1. CO_2 microbubbles production

Citric acid solution was obtained by dissolving 2.1 g $C_6H_8O_7{\cdot}H_2O$ (Kermel, China) in 40 ml deionized distilled water (d.d. water). Sodium bicarbonate solution was obtained by dissolving 2.52 g $NaHCO_3$ (SCRC, China) in 40 ml d.d. water. CO_2 gas was created through the chemical reaction between sodium bicarbonate solution and citric acid solution. CO_2 microbubbles were produced using two syringes and a three-way stopcock (Fig. 1). 1 ml sodium bicarbonate solution and 1 ml citric acid solution were separately placed in two 10 ml syringes, and then the two solutions were mixed. More than 10 ml CO_2 gas was generated. The CO_2 gas was exhausted until 10 ml remained. Then the remaining 10 ml CO_2 gas was evenly mixed with 3 ml egg white through 100 passages between the two syringes using the stopcock as a connector.

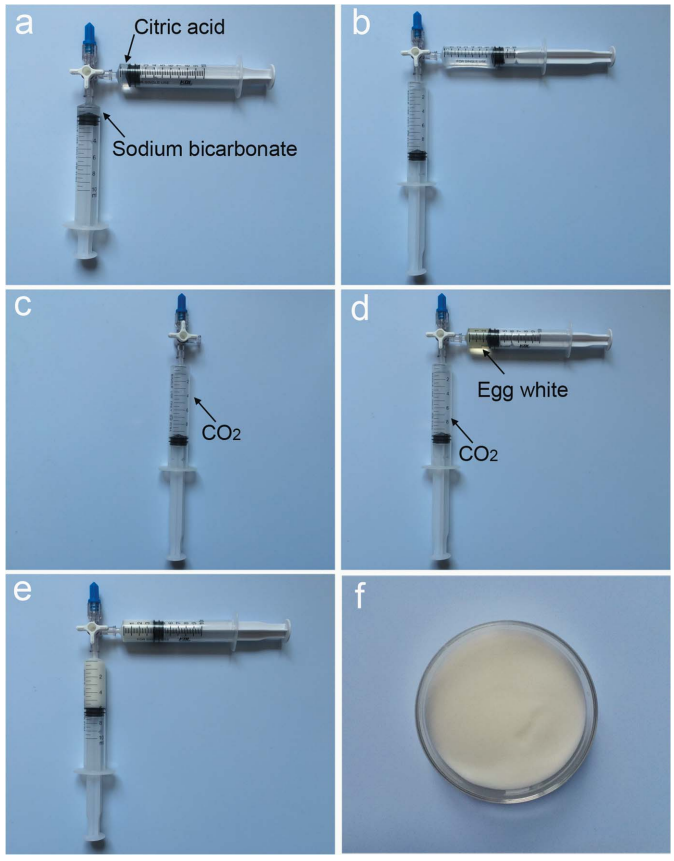

Figure 1
CO_2 microbubbles production with a three-way stopcock. (*a*) 1 ml sodium bicarbonate solution and 1 ml citric acid solution were separately placed in two 10 ml syringes. (*b*) The two solutions were mixed to generate CO_2 gas. (*c*) 10 ml generated CO_2 gas was utilized. (*d*) 3 ml egg white was prepared. (*e*) CO_2 gas and egg white were mixed through 100 passages between the two syringes using the stopcock as a connector. (*f*) The generated CO_2 microbubbles.

2.2. SR parameters

Imaging was performed at the BL13W1 beamline at Shanghai Synchrotron Radiation Facility in China, a third-generation light source based on a 3.5 GeV storage ring. The beamline covered an energy range from 8 to 72.5 keV. The energy resolution ($\Delta E/E$) was less than 5×10^{-3}. Pre-filtered synchrotron X-ray beams were monochromated using a double-crystal monochromator with Si(111) and Si(311) crystals. The transmitted X-rays were captured by a 100 µm-thick $CdWO_4$ cleaved single-crystal scintillator and converted to visible images. Samples were placed 34 m downstream of the synchrotron source. A detector (Hamamatsu, Japan) with a resolution of 3.25 µm was used for acquiring images. The sample-to-detector distance (SDD) was changeable with a range of 8 m. According to previous research in our experimental hutch (Xiao *et al.*, 2005), an energy of 19 keV was chosen for PCI. For comparison, ACI was also performed at 19 keV. Imaging was performed with an exposure time of 1 s. A diagram of the setup is presented in Fig. 2.

2.3. *In vitro* SR of CO_2 microbubbles

The CO_2 microbubbles were placed in a plastic straw. The straw was placed horizontally and perpendicular to the SR beams. ACI and PCI of the CO_2 microbubbles were performed using identical imaging parameters except for the SDDs (1 cm and 30 cm, respectively). The distance was changed by moving the detector on a rail. A PCI time course of the CO_2 microbubbles was performed at the same position in the plastic straw.

2.4. Animals and surgical procedure

The experiment was performed in accordance with the guidelines for the care and use of laboratory animals of Shanghai Jiao Tong University (SJTU). The experimental protocols were approved by the Institutional Animal Care and

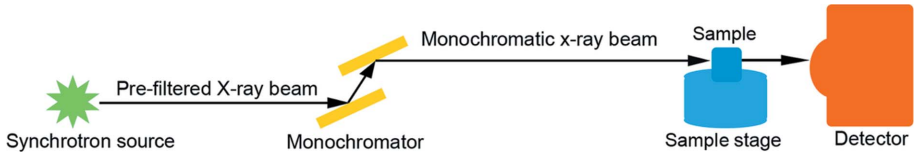

Figure 2
Experimental set-up. Pre-filtered synchrotron X-ray beams were monochromated by a double-crystal monochromator. The SDD had a changeable range of 8 m.

Use Committee (IACUC) and the Bioethics Committee of the School of Medicine, SJTU. Six 6-week-old male Sprague Dawley rats were bought from the Animal Center, CAS, Shanghai, China. The rats were housed in a pathogen-free environment and had free access to water and a normal diet. The rats were anesthetized with ketamine (100 mg kg^{-1}) and xylazine (10 mg kg^{-1}) intraperitoneally. A mid-line abdominal incision was performed on the rats after anesthesia. The main portal trunk was dissected, and then punctured with a thin PE-50 catheter through the mid-line laparotomy. Part of the hepatic lobe was bent so that it protruded from the abdomen in order to obtain a projection image of the liver. 1 ml CO_2 microbubbles solution was injected into the portal system through the catheter.

2.5. *In vivo* PCI and ACI for showing PVE with CO_2 microbubbles

PCI and ACI of PVE were performed using identical imaging parameters except for the SDDs (30 cm and 1 cm, respectively). Three rats were used for PCI. PCI was performed at 2 and 30 min after injection of the the CO_2 microbubbles. The other three rats were used for ACI. For comparing with PCI, ACI was performed at 30 min after injection.

3. Results

3.1. Characteristics of CO_2 microbubbles

The CO_2 microbubbles were spherical particles with smooth surfaces (Fig. 3). The diameter of most of the CO_2 microbubbles was limited to 200 µm. The CO_2 microbubbles were poorly observed on the absorption image obtained with an SDD of 1 cm [Figs. 4(*a*) and 4(*b*)]. After adjusting the distance to 30 cm, we were able to noticeably visualize the CO_2 microbubbles on the phase contrast image [Figs. 4(*c*) and 4(*d*)]. PCI was also performed with a SDD of 30 cm, see Fig. 5.

Figure 3
Optical micrograph of the CO_2 microbubbles. The bubbles were spherical and their surfaces were smooth.

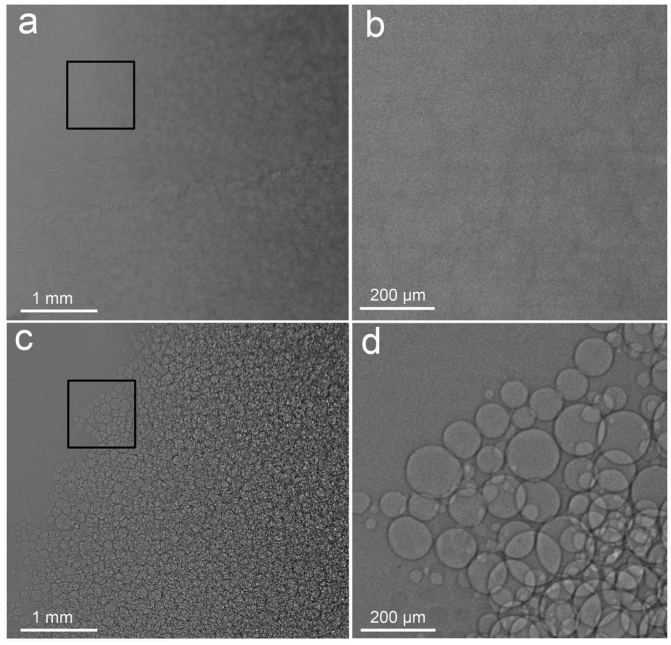

Figure 4
SR images of CO_2 microbubbles with two SDDs of 1 cm (*a*) and 30 cm (*c*). Panels (*b*) and (*d*) show magnified images of the region in the black boxes in (*a*) and (*c*), respectively. The CO_2 microbubbles could be clearly visualized on the phase contrast image (*d*), but not on the absorption contrast image (*b*). The images were obtained at an energy of 19 keV. The pixel size was 3.25 µm × 3.25 µm. The exposure time was 1 s.

The images obtained at the same position showed that CO_2 microbubbles gradually dissolved over time, and the diameter of the remaining CO_2 microbubbles increased. The overlapping microbubbles made it difficult to distinguish individual spheres to assess contrast clarity. This finding indicated that moderate microbubbles might create better contrast than excessive microbubbles. There were still many CO_2 microbubbles remaining at 30 min, indicating a relatively stable characteristic of the microbubbles.

3.2. *In vivo* PCI and ACI of PVE

Blood-filled hepatic portal veins could not be imaged at all by PCI (SDD of 30 cm) before injection of the CO_2 microbubbles (Fig. 6*a*). PCI exploited the differences in the refractive index and enabled clear revelation of the portal vein system at 2 min after the microbubble injection [Figs. 6(*b*) and 6(*c*)]. The portal vein could still be embolized at 30 min after injection (Fig. 6*d*). Compared with ACI (SDD of 1 cm), PCI provided a clearer visualization of the portal vein embolized with CO_2 microbubbles (Fig. 7).

4. Discussion

In order to avoid postoperative liver insufficiency, PVE is clinically employed to stimulate growth of the non-embolized liver segment (van Lienden *et al.*, 2013). Knowing the distribution of embolic agents is essential for making a correct embolization. The efficiency of new PVE methods is

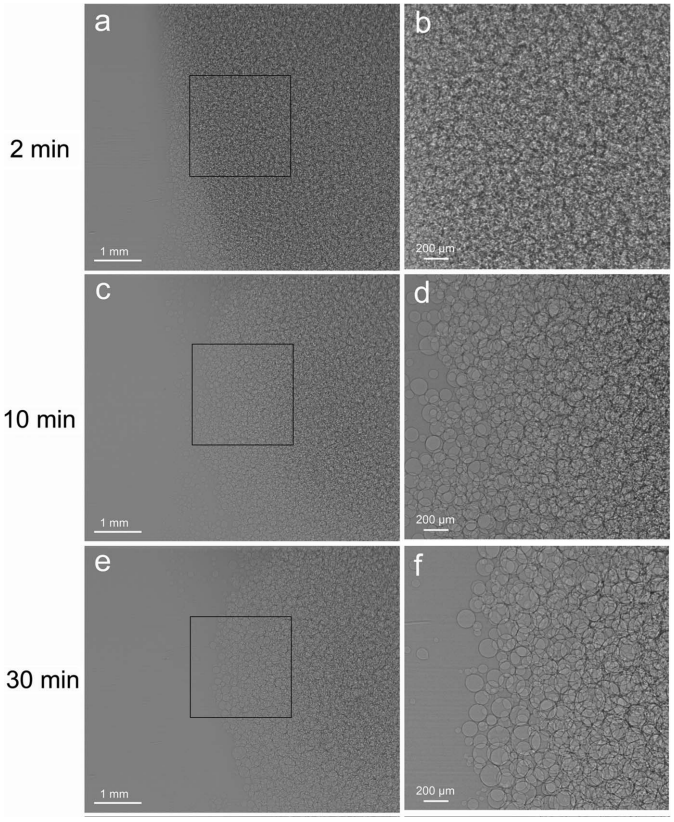

Figure 5
Time course of PCI of CO_2 microbubbles at the same position in a plastic straw. The times after CO_2 microbubbles production are shown on the left. Panels (*b*), (*d*) and (*f*) are magnified images of the regions in the black boxes in (*a*), (*c*) and (*e*), respectively. Note that CO_2 microbubbles gradually dissolve, and the remaining CO_2 microbubbles become larger. The images were obtained at an energy of 19 keV, the pixel size was 3.25 µm × 3.25 µm, the exposure time was 1 s and the SDD was 30 cm.

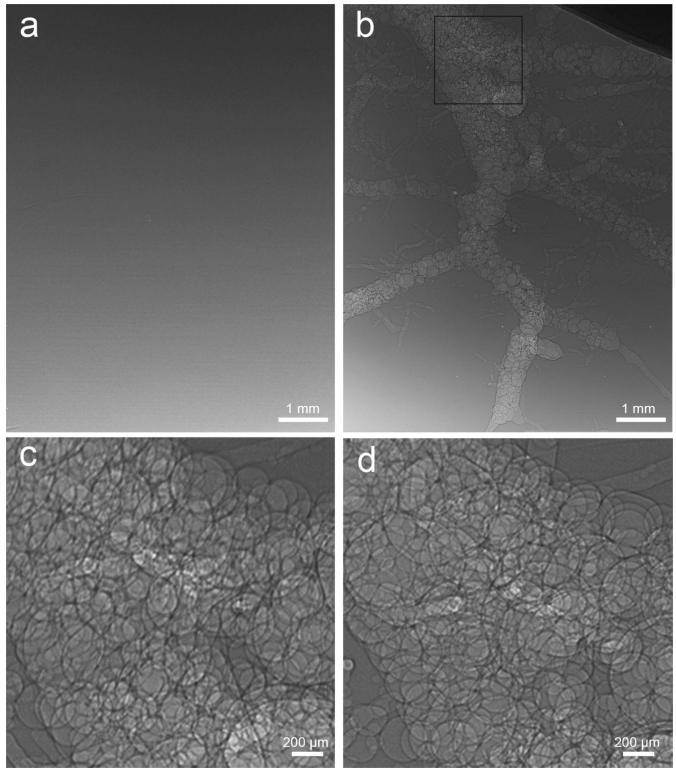

Figure 6
PCI of rat portal veins before and after CO_2 microbubbles injection. Panel (*c*) is a magnified image of the black boxed region in (*b*). Note that no vessels could be detected before CO_2 microbubbles injection (*a*), and the portal veins could be visibly revealed at 2 min (*c*) and 30 min (*d*) after injection. The images were obtained at an energy of 19 keV, the pixel size was 3.25 µm × 3.25 µm, the exposure time was 1 s and the SDD was 30 cm.

commonly first tested in animal models. Therefore, the mechanism and pathophysiological changes can be studied safely before their clinical application. PCI cannot be oriented for clinical use at the present stage; however, it is considered promising for use in animal imaging.

CO_2 gas is considered as a safe contrast agent for clinical applications (Cho & Hawkins, 2008). CO_2 gas can also be applied to clearly visualize fine vessels by PCI (Lundström *et al.*, 2012). Microbubbles have been developed to enhance the contrast in ultrasound (Claudon *et al.*, 2008). In addition, microbubbles have been considered as suitable contrast agents for PCI (Millard *et al.*, 2015). In this study, we turned CO_2 gas into CO_2 microbubbles. The particle size of the homemade CO_2 microbubbles ranged from several micrometers to more than 100 µm in diameter. Some microbubbles with sizes larger than fine vessels could not pass through the fine vessels, thus stopping the perfusion. The shell of the CO_2 microbubbles was formed by egg white, which had significant viscosity to reduce the flowability of the CO_2 microbubbles. Therefore, the blood flow could be notably interrupted by blocking the portal veins.

ACI principally reflects the difference of the density between the adjacent tissues. Because the low-density CO_2 microbubbles absorbed the synchrotron beam weakly, microbubbles could be minimally detected with ACI (Fig. 4*b*). Besides absorption, phase contrast is another important characteristic of SR (Lewis, 2004; Tang *et al.*, 2011). According to the imaging principles of in-line PCI, phase and absorption contrast information can be adjusted and tuned by changing the SDD (Snigirev *et al.*, 1995; Wilkins *et al.*, 1996). The phase

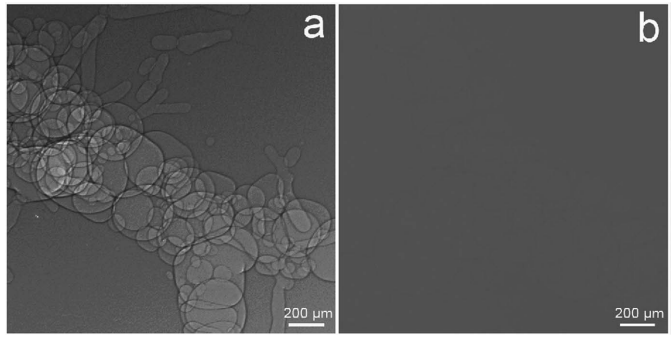

Figure 7
PCI and ACI of PVE. Both PCI and ACI were performed at 30 min after the CO_2 microbubbles injection. Note the embolized portal vein with CO_2 microbubbles was more visibly revealed by PCI (*a*) than ACI (*b*). The images were obtained at an energy of 19 keV, the pixel size was 3.25 µm × 3.25 µm, the exposure time was 1 s and the SDDs were 1 cm and 30 cm for ACI and PCI, respectively.

contrast effects become noticeable when the SDD increases (McDonald *et al.*, 2009). The different refractive index between CO_2 microbubbles and their surroundings can create a significant phase shift to improve the image contrast in PCI (Lee *et al.*, 2014). After the CO_2 microbubbles were delivered through the main portal trunk into the portal system, the blood was replaced by the microbubbles. Compared with the blood–portal vein wall, the CO_2-microbubbles–portal vein wall created more significant phase shifts, which made the boundaries highly observable. Therefore, the CO_2-microbubbles-filled portal veins could be clearly delineated in PCI [Figs. 6(*b*)–6(*d*)]. In contrast, due to the weak absorption difference between the CO_2 microbubbles and the portal vein wall, the embolized portal vein was poorly shown by ACI (Fig. 7*b*).

In summary, this preliminary research suggests that home-made CO_2 microbubbles are potential embolic agents with certain stability for PVE. PCI can help to visibly show the distribution of low-absorption CO_2 microbubbles and evidently identify the embolized liver segment. This novel modality can be first applied for preclinical PVE research in animal models before its realistic clinical diagnosis by PCI.

Funding information

This research was supported by National Science Foundation of China (grants 81471808, 81271740 and 81301347), Nation Basic Research Program of China (973 Program 2010CB834305), and Shanghai Jiao Tong University Med-Science Cross Research Foundation (YG2013MS30).

References

Bravin, A., Coan, P. & Suortti, P. (2013). *Phys. Med. Biol.* **58**, 1–35.
Cho, K. & Hawkins, I. F. (2008). *Clin. Radiol.* **54**, 842–844.
Claudon, M., Cosgrove, D., Albrecht, T., Bolondi, L., Bosio, M., Calliada, F., Correas, J. M., Darge, K., Dietrich, C., D'Onofrio, M., Evans, D. H., Filice, C., Greiner, L., Jäger, K., de Jong, N., Leen, E., Lencioni, R., Lindsell, D., Martegani, A., Meairs, S., Nolsøe, C., Piscaglia, F., Ricci, P., Seidel, G., Skjoldbye, B., Solbiati, L., Thorelius, L., Tranquart, F., Weskott, H. P. & Whittingham, T. (2008). *Ultraschall Med.* **29**, 28–44.
Furrer, K., Tian, Y., Pfammatter, T., Jochum, W., El-Badry, A. M., Graf, R. & Clavien, P. A. (2008). *Hepatology*, **47**, 1615–1623.
Laperle, C. M., Hamilton, T. J., Wintermeyer, P., Walker, E. J., Shi, D., Anastasio, M. A., Derdak, Z., Wands, J. R., Diebold, G. & Rose-Petruck, C. (2008). *Phys. Med. Biol.* **53**, 6911–6923.
Lee, S. J., Park, H. W. & Jung, S. Y. (2014). *J. Synchrotron Rad.* **21**, 1160–1166.
Lewis, R. A. (2004). *Phys. Med. Biol.* **49**, 3573–3583.
Lienden, K. P. van, van den Esschert, J. W., de Graaf, W., Bipat, S., Lameris, S., van Gulik, T. M. & van Delden, O. M. (2013). *Cardiovasc. Intervent. Radiol.* **36**, 25–34.
Lundström, U., Larsson, D. H., Burvall, A., Scott, L., Westermark, U. K., Wilhelm, M., Arsenian Henriksson, M. & Hertz, H. M. (2012). *Phys. Med. Biol.* **57**, 7431–7441.
McDonald, S. A., Marone, F., Hintermüller, C., Mikuljan, G., David, C., Pfeiffer, F. & Stampanoni, M. (2009). *J. Synchrotron Rad.* **16**, 562–572.
Miklos, R., Nielsen, M. S., Einarsdóttir, H., Feidenhans'l, R. & Lametsch, R. (2015). *Meat Sci.* **100**, 217–221.
Millard, T. P., Endrizzi, M., Everdell, N., Rigon, L., Arfelli, F., Menk, R. H., Stride, E. & Olivo, A. (2015). *Sci. Rep.* **5**, 12509.
Omichi, K., Yamashita, S., Cloyd, J. M., Shindoh, J., Mizuno, T., Yun, S. C., Conrad, C., Aloia, T. A., Vauthey, J. N. & Tzeng, C. W. D. (2017). *J. Gastrointest. Surg.* doi:10.1007/s11605-017–3467-1.
Snigirev, A., Snigireva, I., Kohn, V., Kuznetsov, S. & Schelokov, I. (1995). *Rev. Sci. Instrum.* **66**, 5486–5492.
Tang, R., Huang, W., Yan, F., Lu, Y., Chai, W. M., Yang, G. Y. & Chen, K. M. (2012). *PLoS One*, **8**, 182.
Tang, R., Xi, Y., Chai, W. M., Wang, Y., Guan, Y., Yang, G. Y., Xie, H. & Chen, K. M. (2011). *Phys. Med. Biol.* **56**, 3503–3512.
Thüring, T., Abis, M., Wang, Z., David, C. & Stampanoni, M. (2014). *Sci. Rep.* **4**, 5198.
Wilkins, S. W., Gureyev, T. E., Gao, D., Pogany, A. & Stevenson, A. W. (1996). *Nature (London)*, **384**, 335–338.
Xiao, T. Q., Bergamaschi, A., Dreossi, D., Longo, R., Olivo, A., Pani, S., Rigon, L., Rokvic, T., Venanzi, C. & Castelli, E. (2005). *Nucl. Instrum. Methods Phys. Res. A*, **548**, 155–162.
Xuan, R., Zhao, X., Hu, D., Jian, J., Wang, T. & Hu, C. (2015). *Sci. Rep.* **5**, 11500.
Zhang, X., Liu, X. S., Yang, X. R., Chen, S. L., Zhu, P. P. & Yuan, Q. X. (2008). *Phys. Med. Biol.* **53**, 5735–5743.